Available online at www.sciencedirect.com
ScienceDirect

Nuclear Science and Techniques 19 (2008) 121–128

NUCLEAR SCIENCE AND TECHNIQUES

Numerical analysis of turbulent mixed convection air flow in inclined plane channel with *k*-*ε* type turbulence model

XIE Zhengrui* YANG Yanhua GU Hanyang CHENG Xu

School of Nuclear Science and Engineering, Shanghai Jiaotong University, Shanghai 200240, China

Abstract Numerical study on turbulent mixed convection in inclined plane channels, from 15˚ to 90˚ (vertical), was carried out to examine the effect of inclination on fluid flow and heat transfer distributions. The turbulent air flows upward or downward into the duct with one wall heated from bottom. Calculation results with several kinds of *k*-*ε* type turbulence models were used to compare the experimental data with those in literatures to determine suitable model. The dependents of Nusselt number on the inclination angle of both the buoyancy-aided and buoyancy-opposed flow are discussed.

Key words Mixed convection, *k*-*ε* model, Turbulence model, Inlined channel

CLC number TK123

1 Introduction

In heat transfer flows, mixed convection, in which the two mechanisms of the forced convection and natural convection are of interactive influence, is encountered frequently in engineering, especially in nuclear power engineering. For example, the upward flow in cooling system for the fuel elements and in the steam generator, and the downward flow of safety injection in emergency of the passive safe PWR AP1000. The cooling ability of such flows directly determines the safety of the reactor.

Over the past decades, much attention has been paid to both laminar and turbulent mixed convection. A number of studies on buoyancy-influenced heat transfer have been reported. Theoretical and experimental studies on both laminar and turbulent mixed convection in vertical tubes have been reviewed[1], and mixed convection in vertical tubes with uniform wall heat flux with relatively low Reynolds number was studied in Ref.[2], in which a correlation expressing fully developed Nusselt number in terms of Grashof number and Reynolds number was proposed to be valid when $1000 \le Re \le 1500$ and $Gr \le 5\times10^7$. And mixed convection in plane channel with different orientations was experimentally studied in Ref.[3], in which the inclination effect on the Nusselt number was shown for both the lower-wall heated and upper-wall heated configuration.

Most attentions so far, however, were paid to vertical tube with uniform heat flux, or a symmetric system. In this paper, we focus on effect of the inclined angle on the heat transfer of plane ducts. A plane channel in inclination is of engineering importance, but it has not been studied in detail. We did a preliminary calculation to determine the parameters. As no data of inclined plane channel are available, several turbulence models were compared with the experimental data of vertical plane channel to determine the most applicable model for buoyancy influenced flow[4]. With the turbulence model, numerical studies were carried out to find influence of the inclination angle on heat transfer.

* Corresponding author. *E-mail address:* xzr_sjtu@sjtu.edu.cn
Received date: 2007-12-10

2 System scheme

The object of study is a 0.4 m (l) ×8 m (h) ×0.04 m (w) passage with changeable inclination from 15° to 90° (Fig.1). A side wall is heated over a length of 5m as indicated in Fig.1, and the opposed wall is not heated.

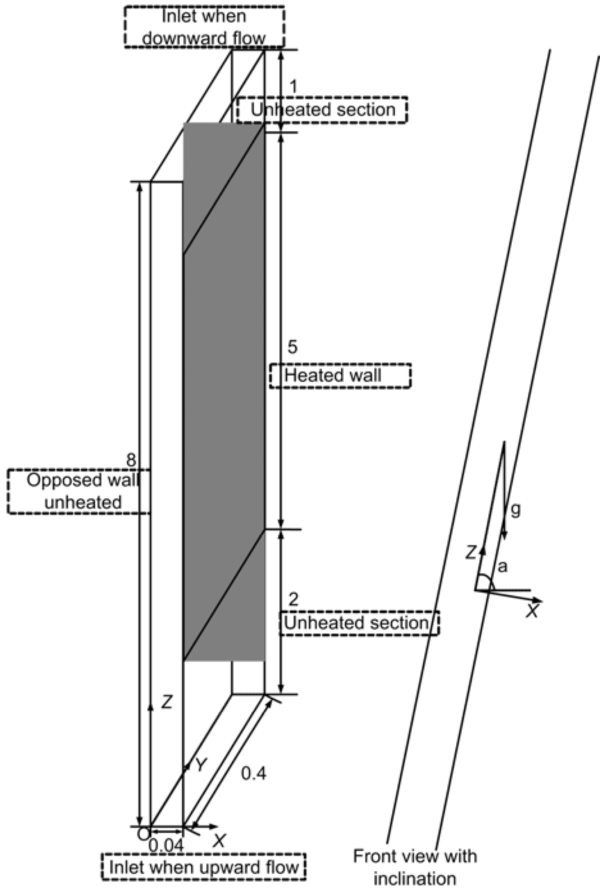

Fig.1 Configuration and dimensions (in meter) of the system studied and the coordination adopted.

3 Turbulence model

Turbulence affects greatly heat transfer of mixed convection, and a correct turbulence model is the key to success of a calculation. The k-ε type model, such as the standard k-ε turbulence model using analytical logarithmic wall-function to bridge the near-wall region, is the most widely used because of its high quality result and the relatively low computer time[5]. Nevertheless, it relies heavily on the assumption of a logarithmic velocity distribution and the validity of local equilibrium of turbulence at this position, which is surely not valid in the position very near the wall.

Since the work of Jones and Launder[6], a number of low-Reynolds k-ε turbulence models were proposed. Jackson and coworkers[1] used the low-Reynolds turbulence model of Launder and Sharma with a ε correction of Yap to calculate a mixed convection in vertical tubes, and found that the model satisfactorily predicted all the experimental data but the descending flow data at high buoyancy influence. In this study, several k-ε type turbulence models, two high-Reynolds-number models, i.e. standard k-ε model and RNG k-ε model, two low-Reynolds-number models, i.e. LB model due to Lam and Bremhorst[7], and a two-layer low-Reynolds-number model, were compared to the experimental data from Ref.[4] to determine the turbulence model applicable to heat transfer in plane channel.

3.1 Standard *k-ε* model

Standard k-ε is widely used in engineering calculations since it was proposed by Launder and Spalding. As the model is based on the assumption of high Reynolds number and cannot be integrated to the wall, the wall function is adopted in the first cell near the wall, as Eq.(1).

$$\begin{cases} \dfrac{dk}{dt} = \dfrac{\partial}{\partial x_j}[(\dfrac{\nu_t}{\sigma_k}+\nu)\dfrac{\partial k}{\partial x_j}] + \nu_t \dfrac{\partial \overline{u}_i}{\partial x_j}(\dfrac{\partial \overline{u}_i}{\partial x_j}+\dfrac{\partial \overline{u}_j}{\partial x_i}) - \beta g_i \overline{u_i'\theta} - \varepsilon \\ \dfrac{d\varepsilon}{dt} = \dfrac{\partial}{\partial x_j}[(\dfrac{\nu_t}{\sigma_\varepsilon}+\nu)\dfrac{\partial \varepsilon}{\partial x_j}] + C_{\varepsilon l}\dfrac{(P_k+G_k)\varepsilon}{k} - C_{\varepsilon 2}\dfrac{\varepsilon^2}{k} \end{cases} \tag{1}$$

where the P_k and G_k is the generation term in k equation due to velocity gradient and buoyancy respectively.

$$\nu_t = C_\mu \frac{k^2}{\varepsilon} \tag{2}$$

$$C_\mu = 0.09, C_{\varepsilon 1} = 1.44, C_{\varepsilon 2} = 1.92, \sigma_k = 1.0, \sigma_\varepsilon = 1.3 \tag{3}$$

3.2 LB low-*Re* model

The low-Reynolds k-ε model chosen in this study is LB model, which is applicable to shear flows, but the ability of this model in mixed convection should be verified. Differing from other low-*Re* models, the model does not include any additional source terms in ε equation. Then, the Neumann boundary condition is imposed on the wall. The model equations are as follows

$$\begin{cases} \dfrac{dk}{dt} = \dfrac{\partial}{\partial x_j}[(\dfrac{\nu_t}{\sigma_k}+\nu)\dfrac{\partial k}{\partial x_j}] - \overline{u_i' u_k'}\dfrac{\partial \overline{u_i}}{\partial x_k} - \beta g_i \overline{u_i'\theta} - \varepsilon - 2\nu\left(\dfrac{\partial k^{\frac{1}{2}}}{\partial x_j}\right)^2 \\ \dfrac{d\varepsilon}{dt} = \dfrac{\partial}{\partial x_j}[(\dfrac{\nu_t}{\sigma_\varepsilon}+\nu)\dfrac{\partial \varepsilon}{\partial x_j}] + C_{\varepsilon 1} f_1 \dfrac{(P_k + G_k)\varepsilon}{k} - C_{\varepsilon 2} f_2 \dfrac{\varepsilon^2}{k} \end{cases} \quad (4)$$

$$\nu_t = C_\mu f_\mu \frac{k^2}{\varepsilon} \quad (5)$$

$$f_\mu = [1-e^{(-0.0165 Re_y)}]^2 (1+\frac{20.5}{Re_t}) \quad (6)$$

$$f_1 = 1 + (0.05/f_\mu)^3, f_2 = 1 - e^{(-Re_t^2)} \quad (7)$$

where $Re_y = \dfrac{k^{1/2} y}{\nu}$, $Re_t = \dfrac{k^2}{\varepsilon\nu}$

3.3 RNG *k*-*ε* model:

The RNG k-ε model has constants that differ from the standard k-ε:

$$C_\mu = 0.0845, C_{\varepsilon 1} = 1.42, C_{\varepsilon 2} = 1.68, \sigma_k = 0.7194, \sigma_\varepsilon = 0.7194$$

The dissipation rate transport equation includes an additional per unit volume source term of

$$S_\varepsilon = \frac{-\rho C_\mu \eta^3 (1 - \dfrac{\eta}{\eta_0})}{1+\beta\eta^3}, \eta = \frac{Sk}{\varepsilon}, S = 2 S_{ij} S_{ji}, \beta = 0.012,\ \eta_0 = 4.38 \quad (8)$$

where S_{ij} is strain rate tensor.

3.4 Yap correction for separation flows

In separated flow the low-*Re* k-ε model gives a far too small dissipation rate, which leads to excessive heat transfer coefficient. Yap *et al*[8] proposed an additional source term to the ε equation in order to remove this deficiency. This correction was adopted by Jackson *et al*[1] for analyzing mixed convection in vertical tubes, and it was used in this comparison study

$$S_\varepsilon = \max[0.83(\frac{l}{l_e}-1)(\frac{l}{l_e})^2 \frac{\varepsilon^2}{k}, 0.0]$$

with

$$l = \frac{k^{3/2}}{\varepsilon}, l_e = 2.5y \quad (9)$$

3.5 Two-layer model[9]

In the near-wall region, the dissipation rate ε is given by

$$\varepsilon = \frac{k^{3/2}}{l_\varepsilon} \quad (10)$$

where $l_\varepsilon = \kappa C_\mu^{-3/4} y/(1+5.3/Re_y)$, $Re_y = k^{1/2} y/\nu$, $C_\mu = 0.09$[10], y is the distance to the nearest wall and κ is the von Karman constant.

The turbulent eddy viscosity $\nu_t = C_\mu k^{1/2} l_\mu$ in this region, with $C_\mu = 0.09$, $l_\mu = \kappa C_\mu^{-3/4} y(1-e^{-25\, Re_y/A_\mu A_+})$, $\kappa = 0.41$, $A_\mu = 50.5$ and $A_+ = 25$[9]. So in the near-wall region, just one transport equation for turbulence kinetic energy k is solved, and, the high-*Re* k-ε model is used outside the region. The location where the one-equation model matched with the two-equation model is $Re_t = 350$.

For selection of the turbulence model, experiment data in Ref.[4] (Table 1) was used to check the effectiveness of turbulence model under the flow condition. Although the configuration in Ref.[4] is a vertical plane passage without inclination, the effectiveness of the turbulence model should be recognized as necessary condition for an inclined one, as no experimental data were available for turbulent mixed convection in inclined plane ducts.

Table 1 Experimental conditions[4]

Case	Flow	M / kg·s^{-1}	T_{b0} / ℃	Q / W·m^{-2}	Bo^*
1	Upward	0.238	18.1	630	4.13×10^{-7}
	Downward	0.235	14.8	628	4.12×10^{-7}
2	Upward	0.109	20.2	1502	9.72×10^{-6}
	Downward	0.111	19.8	1506	1.08×10^{-5}
3	Upward	0.057	18.6	449	3.11×10^{-5}
	Downward	0.055	16.3	449	3.62×10^{-5}
4	Upward	0.056	20.2	1354	8.06×10^{-5}
	Downward	0.053	19.3	1351	1.03×10^{-4}

The standard k-ε model, RNG k-ε model, Lam-Bremhorst low-Reynolds k-ε model and two-layer k-ε model were used to calculate Case 3 in Table 1, which is recognized as a typical mixed convection configuration. Both the velocity profile and the Nusselt number were compared with the experimental data. Because the *k*-*ε* type turbulence models are concerned with this study, the comparison of Reynolds stress is beyond the scope of this paper.

It can be seen from the comparison (Figs.2 and 3) that in the upward flow, except the two-layer model, all the models give no satisfactory velocity profile. LB model and LB model with Yap correction give too high velocity near the heated wall. The standard and RNG *k*-*ε* models give higher velocity near the heated wall, too, probably because of the higher Nusselt number estimated. All the models give the right tendency of Nusselt number distribution, but the standard and RNG *k*-*ε* models give too high Nusselt number compared to the experimental data along the axial direction. However, for the other models, two-layer model gives better result in low *x/D*e region, and the LB model and LB model with Yap correction give better result in the high *x/D*e region. For the downward flows, the two-layer model gives the acceptable Nusselt number, but results of the standard and RN*G* *k*-*ε* models are too large and results of the LB model and LB model with Yap correction are wrong in the low *x/D*e region. Above all, the two-layer model is the only one with acceptable result in both upward and downward flow.

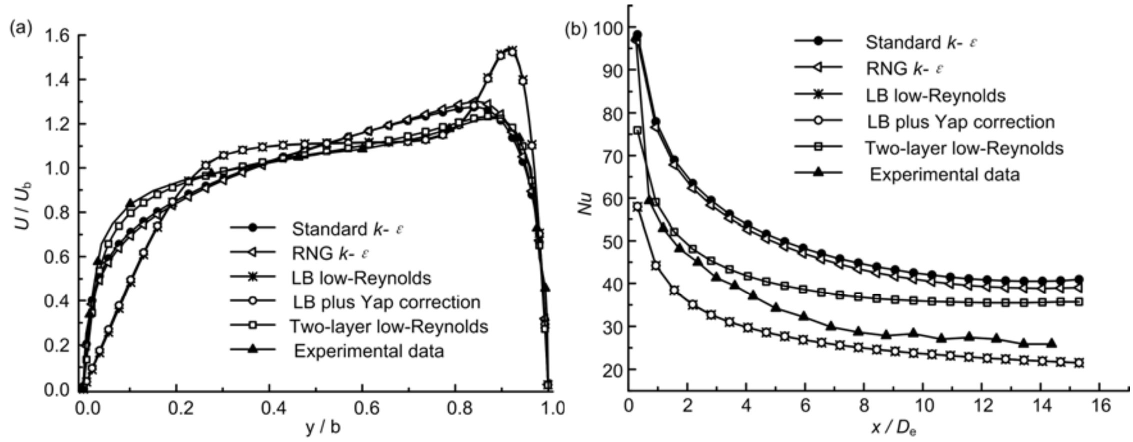

Fig.2 Upward flow velocity profile (a) and Nusselt distribution (b) of Case 3 in Table 1 by different turbulence models.

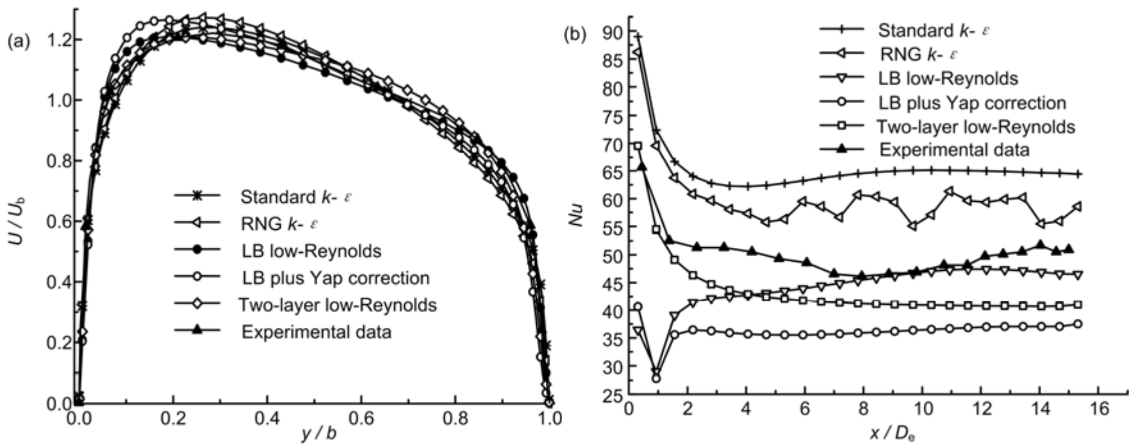

Fig.3 Downward flow velocity profile (a) and Nusselt distribution (b) of Case 3 in Table 1 by different turbulence models.

The other cases in Table 1 were calculated with the two-layer model, and the results (Figs.4 and 5) show that the turbulence model is effective in the wide range of Bo^* number of mixed convection, though with obvious differences from experimental data, especially in the downward flow case with high buoyancy influence. Therefore, the two-layer *k*-*ε* model was selected for studying the inclined ducts.

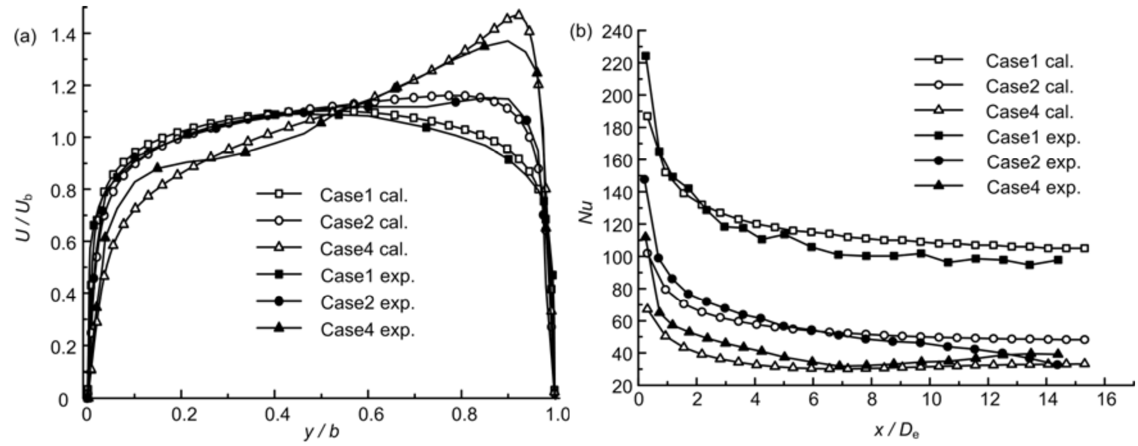

Fig.4 Upward flow velocity profile (a) and Nusselt distribution (b) of Case 1, 2 and 4 in Table 1 by different turbulence models.

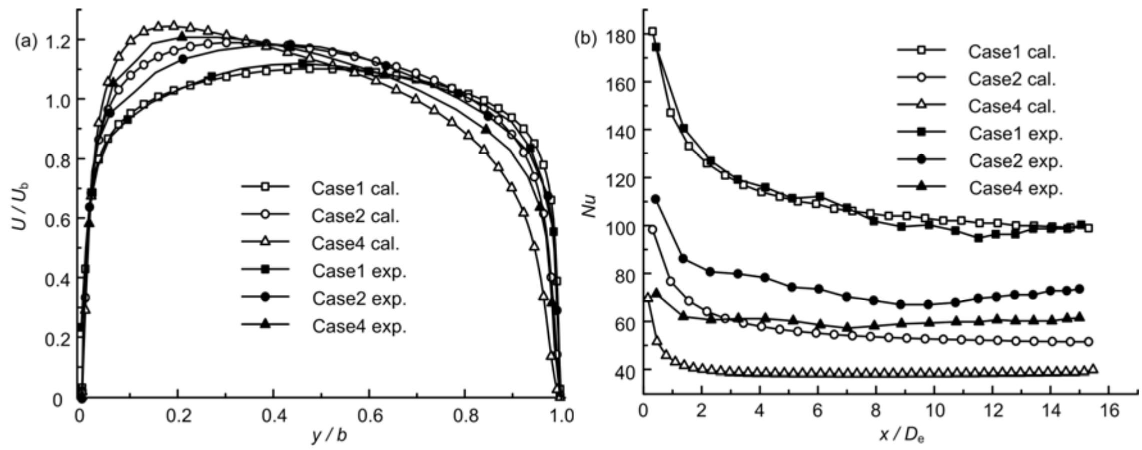

Fig.5 Downward flow velocity profile (a) and Nusselt distribution (b) of Cases 1, 2 and 4 in Table 1 by different turbulence models.

4 Results and discussion

Because the aspect ratio in Fig.1 is 10:1, in the mid plane of the flow a two-dimensional condition would be approached, and a two-dimensional calculation was carried out. The results are given in Table 2. The Nusselt number distribution in different axial position is shown in Fig.6.

Table 2 Cases calculated at 20℃

Case	Flow	V_{in} / m·s^{-1}	Q / W·m^{-2}	Re	Gr^*	Bo^*
1	Upward	1	250	5181.4	6.870×10^{7}	1.733×10^{-5}
	Downward	1	250	5181.4	6.870×10^{7}	1.733×10^{-5}
2	Upward	1	500	5181.4	1.374×10^{8}	3.467×10^{-5}
	Downward	1	500	5181.4	1.374×10^{8}	3.467×10^{-5}
3	Upward	1	1000	5181.4	2.748×10^{8}	6.934×10^{-5}
	Downward	1	1000	5181.4	2.748×10^{8}	6.934×10^{-5}
4	Upward	0.5	500	2590.7	1.374×10^{8}	3.724×10^{-5}
	Downward	0.5	500	2590.7	1.374×10^{8}	3.724×10^{-5}

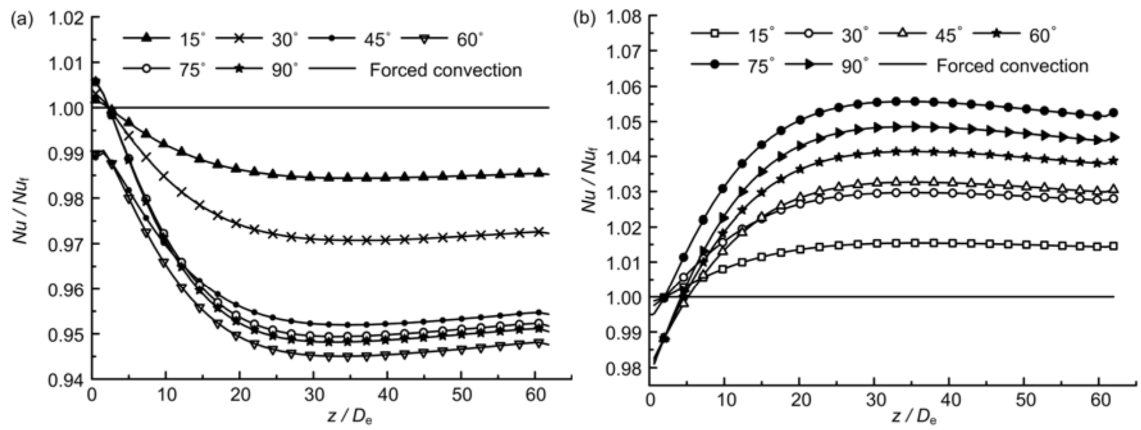

Fig.6 Nusselt number distribution for Case 1 in Table 2 (a) upward flow and downward flow (b).

The Nusselt number of Case 1 upward flow is smaller than that in pure forced convection condition in all the axial positions. This is referred by many authors as impaired heat transfer. Along the axial direction, the Nusselt number decreases quickly with a minimum at z/De≈30. The minimum value decreases slightly with increasing inclination, getting the smallest minimum Nusselt number at θ=60°. In the downward flow condition, enhanced heat transfer occurs in all angles along the axial direction. And peak value of the Nusselt number at z/De≈30, too, reaching the highest peak value at θ=75°.

The results of Case 2 are shown in Fig.7. The inlet velocity is 1m·s^{-1}, but the heat flux increases to 500W/m^2, hence a stronger buoyancy influence, which leads to increased deviation of heat transfer from forced convection. The minimum and maximum value of Nu/Nu_f in the upward flow is about 0.92 and 1.10, respectively, rather than 0.945 and 1.055 in Case 1. In the upward flow, with increasing inclination, the axial position of the Nusselt number extreme moves towards the start point of the heated section. The Nusselt number increases at 60°~75°, but decrease then. From 75° to 90°, the Nusselt number climbs quickly to a peak value at z/De≈40 and decreases slowly along the axial direction. In the downward flow, except for the amplitude of Nusselt number, its deviation from forced convection is almost similar to that in Case 1. However, the difference from 75° to 90° is smaller than Case 1.

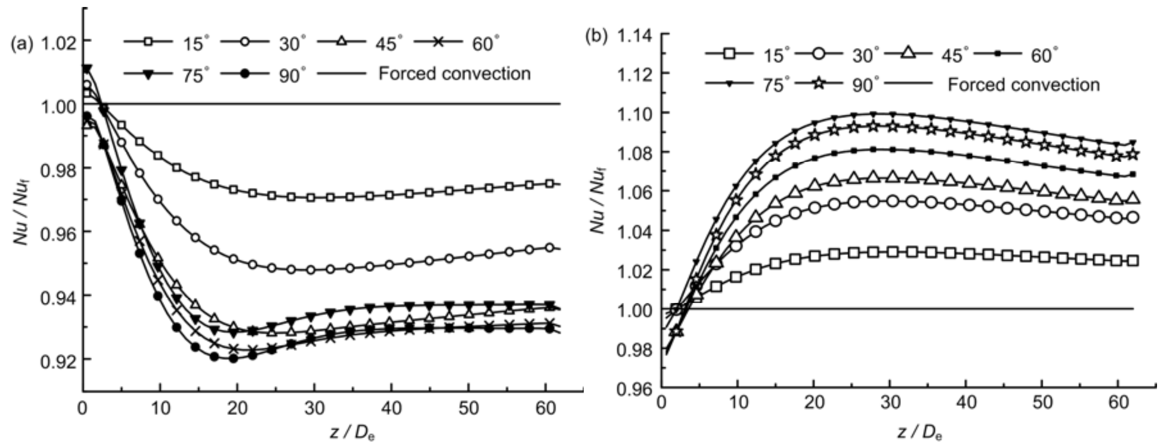

Fig.7 Nusselt number distribution for Case 2 in Table 2, upward flow (a) and downward flow (b).

In Case 3 (Fig.8), the inlet velocity of the channel remaines the same and the heat power increases to 1000 W/m^2, the buoyancy influence is further enhanced. The results of downward flow show little difference with Case 2, except for the amplitude of deviation and the difference from 75° to 90°. But for the upward flow, with increasing inclination angle, the second extremum of Nusselt number occurs at θ=45°, rather than 75° in Case 2.

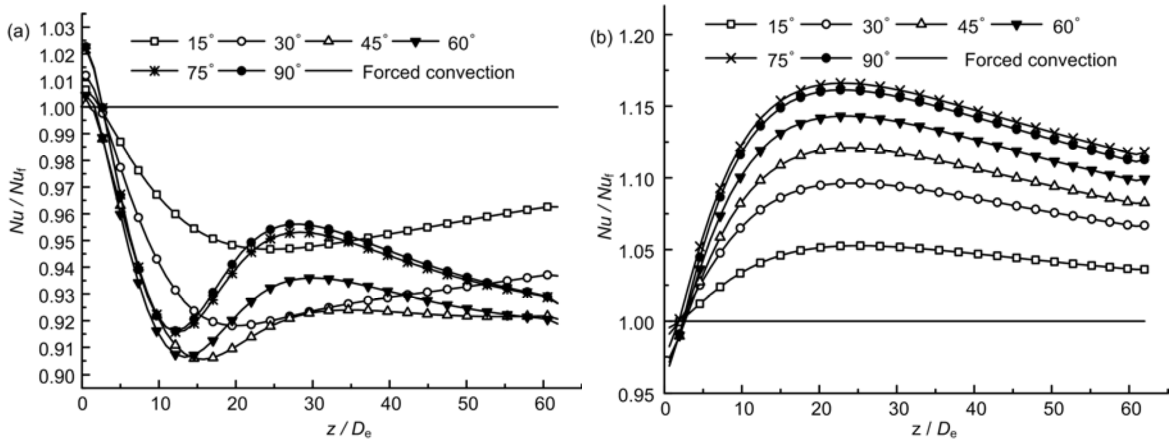

Fig.8 Nusselt number distribution for Case 3 in Table 2, upward flow (a) and downward flow (b).

The inlet velocity of Case 4 is reduced to 0.5 m·s^{-1}. Its buoyancy parameter Bo^* is defined as Ref.[1], the largest among the four cases, so the buoyancy influence is the most significant, as can be seen in Fig.9. While the downward flow does not differ much from the other cases, the heat transfer of upward flow differs from the other cases. Except for θ=15°, the Nusselt numbers are greater than that in forced convection condition. Agreeing with Ref.[1], in which the buoyancy parameter Bo^* is greater than a critical value, and the heat transfer is enhanced in upward flow in vertical tubes. The upward flow enhancement in Case 4 is so strong that the Nu/Nu_f is very close to the downward flow.

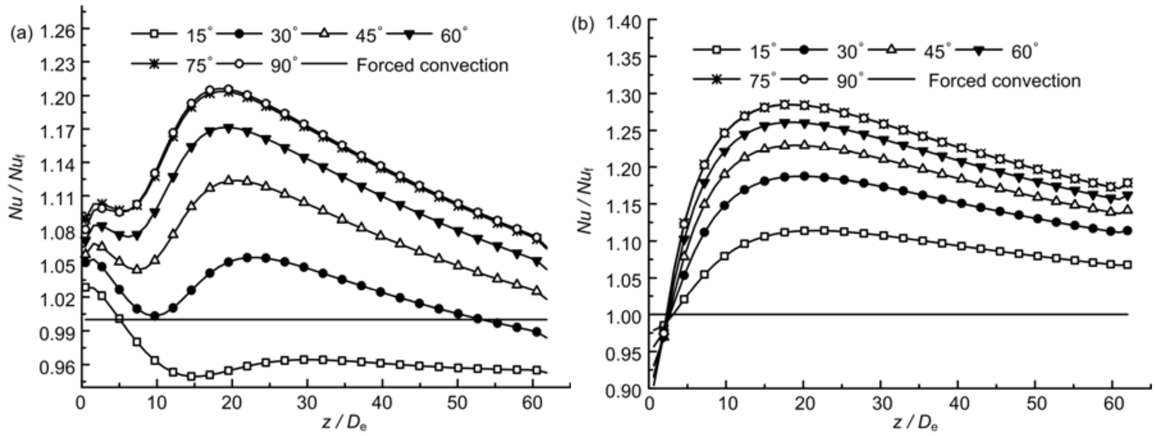

Fig.9 Nusselt number distribution for Case 4 in Table 2, upward flow (a) and downward flow (b).

5 Conclusion

Using experimental data from Ref.[8], a numerical study on inclined plane channel was done to verify turbulence models for turbulent mixed convection in plane channel. It was found that, unlike turbulence models of standard k-ε model, RNG k-ε model, LB low-Reynolds-number model and LB model with Yap correction, the two-layer k-ε model gave acceptable results of the velocity and heat transfer.

The inclined plane channel was studied with the two-layer k-ε model. The results show that with increasing buoyancy influence, which is indicated by Bo^* number, the inclined angle makes greater influence. Generally, in the downward flows, heat transfer enhancement occurs in all the cases, and the Nusselt number varies more quickly when Bo^* is larger. The greatest Nusselt number is at θ=75° in all cases, but the difference from 75° to 90° is reduced with increasing Bo^*.

In the upward flows, when Bo^* is relatively small, heat transfer impairment occurs along the whole axial direction, and at $z/De\approx30$ the Nusselt number reaches its minimum value. With increasing Bo^*, a second extremum appears, which takes place earlier in larger inclinations. By further increasing Bo^*, the position of the minimum value moves towards the starting of heating and the second extremum becomes more obvious. After a critical Bo^*, the heat transfer enhancement occurs, which takes place earlier in larger angles, too.

The results show that the inclination of the plane channel has a great influence on heat transfer, especially under high buoyancy influenced condition.

Nomenclatures

b distance between the unheated and heated walls
Bo^* buoyancy parameter, $Gr^*/Re^{3.425}Pr^{0.8}$
C_p specific heat at constant pressure
D_e equivalent diameter, 2b
Gr^* Grashof number based on wall heat flux, $g\beta qD_e^4/(v^2k)$
g gravity
h heat transfer coefficient, $q/(T_w-T_b)$
k thermal conductivity or turbulent kinetic energy
Nu Nusselt number, hD_e/k
Nu_f Nusselt number of forced convection flow
Pr Prandtl number, $\mu C_p/k$
P_k the generation term due to velocity gradient in k equation
G_k the generation term due to buoyancy in k equation
Re Reynolds number, U_bD_e/v
q wall heat flux
T_w wall temperature
T_b bulk fluid temperature
U axial component of time mean local velocity
U_b bulk fluid velocity
x axial coordinate measured from start of heating in Ref.[1] or the transverse coordinate
y y coordinate in Fig.1
z z coordinate in Fig.1 or axial coordinate measured from start of heating
β thermal expansion coefficient
μ dynamic viscosity
v kinematic viscosity, μ/ρ
v_t turbulent eddy viscosity
ρ density
ε turbulent dissipation rate
θ the inclined angle of the channel
C_μ, $C_{\varepsilon1}$, $C_{\varepsilon2}$, σ_k, σ_ε constants in k-ε models
f_μ, f_1, f_2 functions used in low-Reynolds k-ε models
Re_y, Re_t local Reynolds number used in low-Reynolds k-ε models
S_ε additional source term in ε equation of *RNG* k-ε model or Yap correction
l_ε, l_μ length scale used in two-layer model in near wall region
A_μ, A_+ constants used in two-layer model
x_i, x_j Cartesian coordinate in the i, j-th direction
S_{ij} strain rate tensor
u_i' fluctuation velocity in the i-th direction
$\overline{u_i}$ averaged velocity in the i-th direction
t time

Subscripts

i,j i, j direction
t turbulent parameter

References

1 Jackson J D, Cotton M A, Axcell B P. Int J Heat Fluid Flow, 1989, **10:** 2-15.
2 Behzadmehr A, Galanis N, Laneville A. Int J Heat Mass Transf, 2003, **46:** 4823-4833.
3 Poškas P. J Eng Phys Thermophys, 1996, **69:** 738-746.
4 Wang J, Li J, Jackson J D, Int J Heat Fluid Flow, 2004, **25:** 420-430.
5 Launder B E, Spalding D B. Comput Methods Appl Mech Engng, 1974, **3:** 269-289.
6 Jones W P, Launder B E. Int J Heat Mass Transf, 1972, **15:** 301-314.
7 Lam C K G, Bremhorst K. J Fluids Engng, 1981, **103:** 456-460.
8 Yap C. Faculty of technology, PhD Thesis. University of Manchester, 1987.
9 Rodi W. AIAA-91-0216. 29th Aerospaces Sciences Meeting, Reno, Nevada, USA, January 7-10, 1991.
10 Cotton M A, Jackson J D, Int J Heat Mass Transf, 1990, **33:** 275-286.
11 Norris L H, Reynolds W C. Report No. FM-10: turbulent channel flow with a moving wavy boundary. Stanford University, Department Mechanical Engineering, 1975.